Short streamers and sparse OBN acquisition: Potential for CCS monitoring?

S. David[1]*, F. Ten Kroode[1], E. Cho[1], M.A.H. Zuberi[1], G. Stock[1], S. Baldock[1], J. Mispel[2], H. Westerdahl[2], M. Thompson[2] and Å. Sjøen Pedersen[2] demonstrate the added value of using the multiples in FWI, deriving a velocity model to migrate the short streamer data, and suggest ways to address limitations encountered when trying to push FWI on sparse nodal data to higher frequencies.

Introduction

The Paris Agreement aims at restraining global warming with efforts to limit the increase in temperature to 1.5°C above the pre-industrial level. Achieving these ambitious targets requires a significant reduction in greenhouse gas emissions, with Carbon Capture and Storage (CCS) emerging as a critical technology. CCS involves capturing CO_2 emissions from industrial sources, transporting it to a storage site, and injecting it into geological formations for long-term storage. For CCS to be effective and gain public and regulatory acceptance, robust monitoring technologies are essential to ensure that the captured CO_2 remains securely stored.

Subsurface monitoring plays a significant role in verifying containment and conformance. It involves tracking the movement of CO_2 within the storage formation to confirm that it stays within that formation and within the licence and behaves as predicted by the reservoir model. Various techniques are available and present benefits and drawbacks (pressure and temperature, well logging, …). Monitoring strategies must be tailored to the specific characteristics of each storage site and technologies need to be adapted accordingly.

As the energy transition progresses, overlaps and conflicts between oil and gas projects, offshore windfarm developments and carbon capture and storage projects will increasingly emerge. In these future congested areas, CCS monitoring will be particularly challenging due to limited space and restricted access for deploying monitoring equipment. Potential interference from other activities will also affect the monitoring solutions (Quirk et al, 2021).

Considering these challenges and starting from technologies that are traditionally used in the oil and gas industry, we wanted to evaluate the potential of using short streamers and free-fall, self-recovering Ocean Bottom Nodes (OBNs) for CCS monitoring in an innovative and cost-effective way. To do this, a field test – financially supported by Equinor and CLIMIT – was carried out at the Sleipner CCS field in the North Sea, where CO_2 has been sequestered and monitored since 1996 (A-K Furre et al., 2016; P. Ringrose, 2018; J. Mispel et al., 2019 and R. Dehghan-Niri et al., 2022). Carbon dioxide has migrated into nine thin sand layers, which need to be imaged at a high enough resolution in order to confirm containment and conformance.

Forty-seven OBNs were deployed on a sparse 500 by 525 m grid (with densification to 100 m along one line) to derive a velocity model to migrate the high-resolution data acquired with the short streamers. Sparse node acquisition faces challenges with high-frequency FWI-based velocity updates due to limited illumination of the subsurface with reflected waves. The approach used to overcome this limitation is to include multiples in the Full Waveform Inversion (FWI), in addition to primary reflections, to constrain the velocity estimation and to provide a higher-resolution FWI-derived velocity model.

In this paper, we show the added value of using the multiples in FWI in order to derive a velocity model to migrate the short streamer data. We also show the limitations encountered when trying to push FWI on sparse nodal data to higher frequencies and suggest future work to address these.

Acquisition set-up

A hybrid streamer and OBN survey was conducted to demonstrate the benefits of two recently developed acquisition technologies: high-resolution mini-streamer acquisition (eXtended

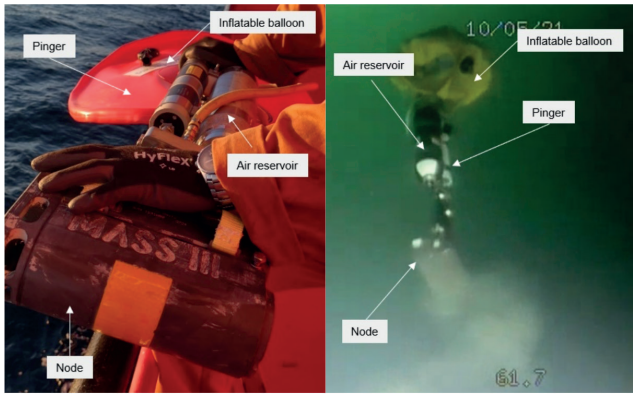

Figure 1 Pictures showing the self-recovery device attached to the OBN. Nodes are simply thrown overboard (left) and recovered by an inflatable balloon lifting the node to the sea surface (right).

[1] TGS ASA | [2] Equinor ASA
* Corresponding author, E-mail: sandrine.david@tgs.com
DOI: 10.3997/1365-2397.fb2024094

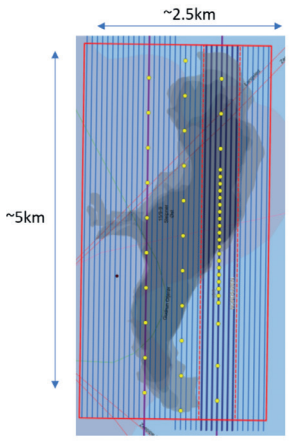

Number of nodes	47
Sparse node grid	500m x 525m
Dense grid inline spacing	100m
Sail-line interval	75m
Shotpoint interval	6.25m (flip-flop)

Figure 2 Acquisition layout. The blue lines are the sail lines for the streamer survey. The yellow dots are the Ocean Bottom Node locations. Grey outlines indicate the CO_2 extension layers.

High Resolution – XHR) (R. Dehghan-Niri et al., 2023) and free-fall, self-recovering OBNs. Two independent datasets were acquired simultaneously, with the OBN dataset complementing the short-streamer dataset by providing long offsets and good S/N at low frequencies for an FWI-based velocity model update.

Minimising the cost of monitoring is obviously very important for CCS projects. To meet this objective, a free-fall approach was used to deploy the nodes. The OBNs were also equipped with a 'pop-up' self-recovery mechanism to optimise retrieval. This has the advantage of accelerating node recovery and eliminating the need for more expensive Remotely Operated Vehicle (ROV) or Node-on-a-Rope (NOAR) solutions. The self-recovery device is made of an inflatable balloon, a pinger and an air reservoir. The system is activated by sending an acoustic signal to the pinger, which triggers a valve on the air reservoir to open, after which the balloon is filled and lifts the node to the sea surface (Figure 1).

To optimise the cost further, a very limited number of nodes was used and deployed on a sparse grid (500 m x 525 m) with denser node spacing of 100 m along one receiver line for testing purposes. Shots recorded by the nodes are the shots fired from the short streamer XHR acquisition, with a shot grid of 6.25-m flip-flop and 75-m sail-line spacing (Figure 2).

Objectives

The aim of the study was two-fold. First, we wanted to evaluate the capabilities of FWI in shallow water, 80 m at Sleipner, and, with sparse nodal data, to produce a velocity model suitable for imaging the short streamer data. Second, we wanted to compare the resolution of FWI images against that of short streamer images.

Sparse node acquisition has limitations, notably in the sampling of the very shallow subsurface which can compromise high-frequency velocity updates. At low frequencies, FWI predominantly relies on diving wave energy where the sparsity of the nodes is not a problem. Estimating a high-resolution velocity model with FWI relies on small angle reflection energy, which is highly sensitive to node spacing. To address these challenges, our approach leverages multiples instead of relying solely on primary reflection data to stabilise and enhance the accuracy of the FWI-derived velocity model. Multiples contain more near-angle information and provide better illumination compared to primary reflections, which could ultimately enable robust and reliable monitoring of CCS sites.

Building a low-frequency velocity model

A 3D initial velocity model volume was derived from 2D data spanning the survey area. The velocity model was calibrated to match the velocity profile of the closest available well information and smoothed to produce a well calibrated velocity model. Two temperature and salinity velocity profiles (TS-dip) were acquired, transcribed and evaluated as function for the water column. For shallow water depth, a single value water velocity was considered sufficient for water column velocity and a velocity of 1492 m/s was selected. The anisotropy model used was a constant delta 3% and epsilon 4.5%.

During acquisition, near field hydrophone (NFH) data were recorded. Applying a single global debubble operator based on the NFH data, showed some jitters and left some residual bubble

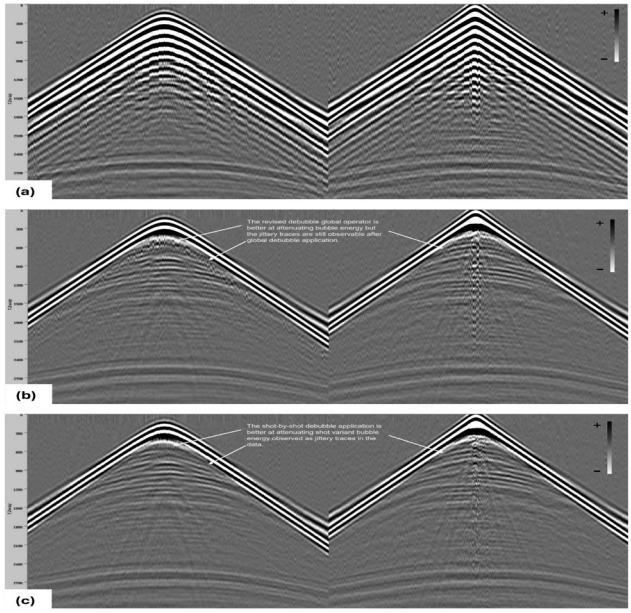

Figure 3 Hydrophone data examples: raw (a), debubble using global derived operator (b), debubble using shot-by-shot derived operators (c)

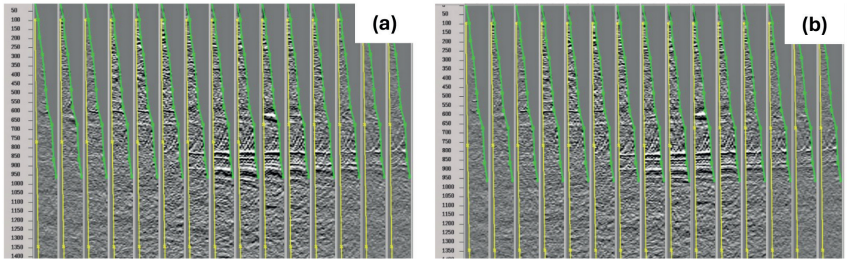

Figure 4 Image gathers of Up-Down deconvolved OBN data: in the initial velocity model (a) and in the 8Hz FWI velocity model (b).

energy, so the NFH data were used to derive individual shot-to-shot operators which provided an improved debubble result (Figure 3).

The hydrophone node data were used to perform FWI utilising both diving wave and reflection energy, in 0-4 Hz, 0-6 Hz and 0-8 Hz frequency bands. An acoustic Dynamic Matching FWI (DM FWI) was used. The DM FWI algorithm addresses the inversion problem by maximising the cross-correlation between the recorded and synthetic data. By dynamically matching these datasets (i.e., matching the amplitude of the synthetic data with that of the field data either by normalisation or by matching the amplitude of the synthetic data to the field data), the algorithm reduces the influence of amplitude, allowing it to minimise kinematic differences during the data-fitting process (Huang et al. 2020 and 2023; Mao et al., 2020). The FWI results were reviewed carefully through data domain QC and pre-stack depth Kirchhoff migration of Up-Down deconvolved OBN data. It was observed that FWI has successfully captured the general background velocity, with common image gathers showing good gather flatness (Figure 4).

Higher-frequency updates: Two approaches

In the past decade, an increasing number of projects have treated multiple reflections as signals for imaging the subsurface, rather than as noise. Imaging with multiples provides improved near-angle illumination, which goes hand-in-hand with enhanced resolution and a wider illuminated area. This is predominantly valid in shallow areas, where multiples illuminate the subsurface at smaller reflection angles than the primaries.

Using the full wavefield in velocity model-building provides similar benefits to those described above for imaging and it is being increasingly used in FWI flows. Using multiples in FWI increases the non-linearity of the inversion problem, meaning that it is easier for inversions to get stuck in a local minima, resulting in cycle-skipping artefacts in the final model. However, use of the full wavefield has the potential to accelerate the full imaging flow by removing the need for the time-consuming pre-processing steps (Figure 5).

Following the two pre-processing workflows, FWI was run in increasing frequency bands from 0-12Hz, 0-15Hz and 0-25Hz using two different data sets as input, namely the Up-Down deconvolved data set and the hydrophone data set with minimal preprocessing (Figure 6).

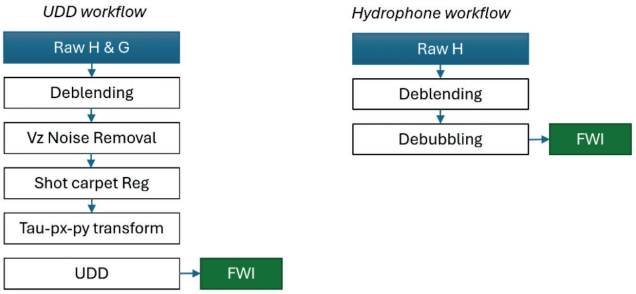

Figure 5 Pre-processing workflow diagrams comparisons.

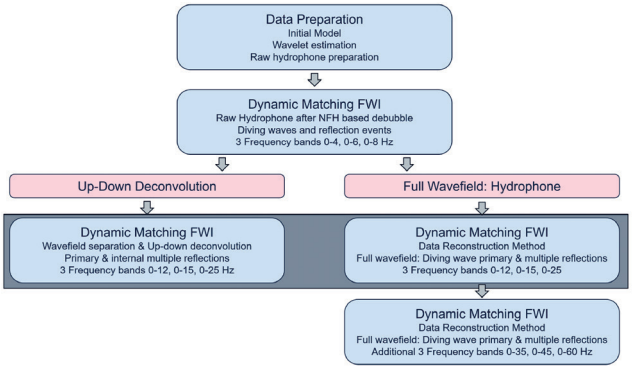

Figure 6 FWI workflows. Comparisons made at 25Hz.

In the first approach, the node data were processed through to Up-Down Deconvolution (UDD), utilising both the hydrophone and vertical geophone components. This process yielded a dataset with surface reflection events, such as ghosts and surface multiples, removed (Figure 7 b). Subsequent FWI can then be run with an absorbing boundary condition in the numerical scheme for forward and backward modelling. It is important to note that UDD assumes a horizontally layered earth, an assumption which will be violated in complex geological settings. However, for the Sleipner case, this assumption is generally valid.

A second approach was based on running FWI on the full-wavefield hydrophone (P) data, with de-bubble only applied (Figure 7 c). In this method, the free surface reflectivity was included in the inversion, and a data reconstruction method (Zuberi et al., 2023) was utilised to mitigate the effects of guided waves and ocean bottom waves, which cannot be explained properly by acoustic modelling.

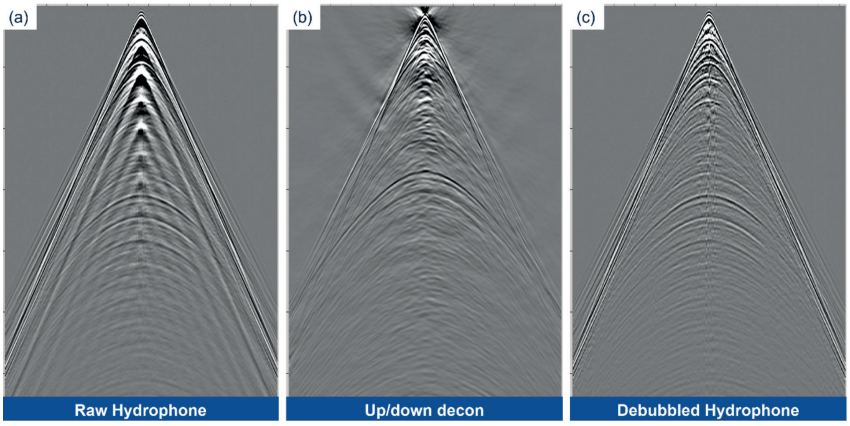

Figure 7 Example of a nodal gather and input data to FWI for the two different routes. Raw Hydrophone data (a), UDD data (b), hydrophone data with debubble applied (c).

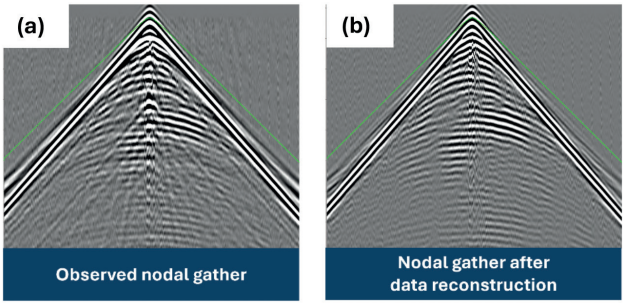

Figure 8 Example of hydrophone nodal gather after the data reconstruction method application. 0-12Hz observed nodal gather (a), 0-12Hz nodal gather after data reconstruction (b).

Data reconstruction methodology

Elastic effects in the near surface can cause a mismatch between the acoustic modelled data and the observed data. In principle, elastic modelling should allow a better match between the modelled and observed data for FWI. In practice, however, the increased computational cost and parameter uncertainty associated with taking more physics into account (several parameters to invert for) can pose serious challenges to FWI. Moreover, since the multiples depend non-linearly on velocity, any discrepancy due to unexplained elastic effects would make inversion with multiples more challenging. We have therefore opted for acoustic FWI in this study.

To mitigate the near-surface elastic effects in a computationally efficient manner, we use the data reconstruction method proposed by Zuberi et. al. (2023). This method reconstructs an acoustic equivalent of the observed data, which is subsequently used in FWI as the observed data. The acoustic equivalent is obtained by matching the observed source gathers (in this study sources and receivers are interchanged for computational efficiency) to the modelled gathers and applying the resulting matching/reconstruction filter to the observed data (Figure 8). As the reconstruction filter is a single filter applied to whole source gather, it does not alter the slopes or curvatures of the events in the data. In other words, by using data reconstruction we can mitigate the elastic effects by absorbing them in the reconstruction filter instead of leaving them in the residual, which can cause spurious updates. This may be more important for multiples due to their non-linear dependence on elastic perturbations. Data reconstruction is an approximate technique to use all data acquired in an elastic earth, including multiples, in an acoustic FWI scheme.

In general, the reconstruction filter can absorb features in the data that are not explained by the modelling, which is like a conventional source inversion. Zuberi et al. (2023) also show that data reconstruction performs source inversion implicitly; that is, the data reconstruction filter is an inverse of the matching filter for conventional source inversion. Therefore, in this study we did not have to perform explicit source inversion/wavelet estimation.

Comparison of FWI results on UDD and 'raw' hydrophone data

Figures 9c and 9d show the velocity models obtained from the two approaches after the 25 Hz update. Figures 9a and 9b are shown for comparison and contain the initial velocity model used and the 8Hz FWI velocity model from the low-frequency

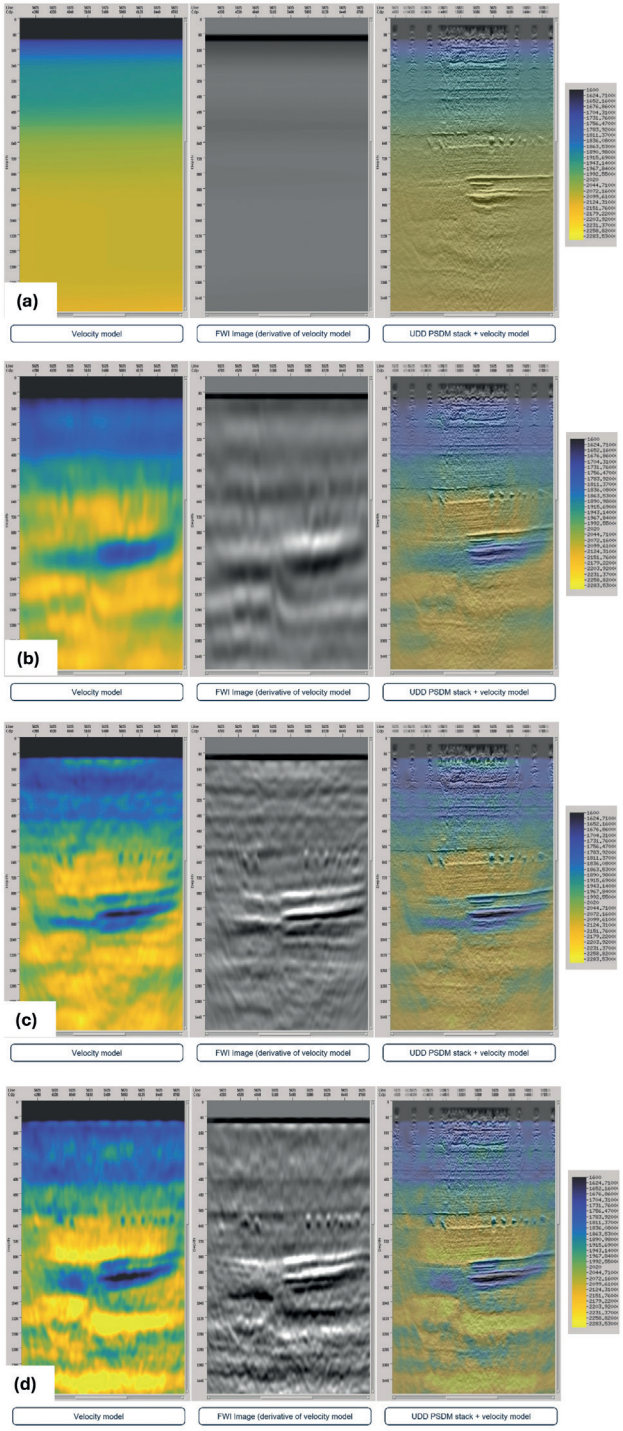

Figure 9 Velocity model (left), FWI image (middle) and KPSDM image (right) obtained in: initial model (a), 8Hz FWI velocity model (b), 25Hz FWI full hydrophone data velocity model (c) and 25Hz FWI UDD data velocity model (d).

update phase. FWI images derived from these velocity models and KPSDM sections derived using these velocity models are also included to help with the comparison and the interpretation of the results. The KPSDM results used for QC and comparisons were derived using the UDD data from the dense node line (inline sections) and the XHR streamer data (depth slices).

A first glance at the results shows that the CO_2 plume has a distinct slow velocity and can be clearly observed in both approaches. However, the UDD result provides less definition

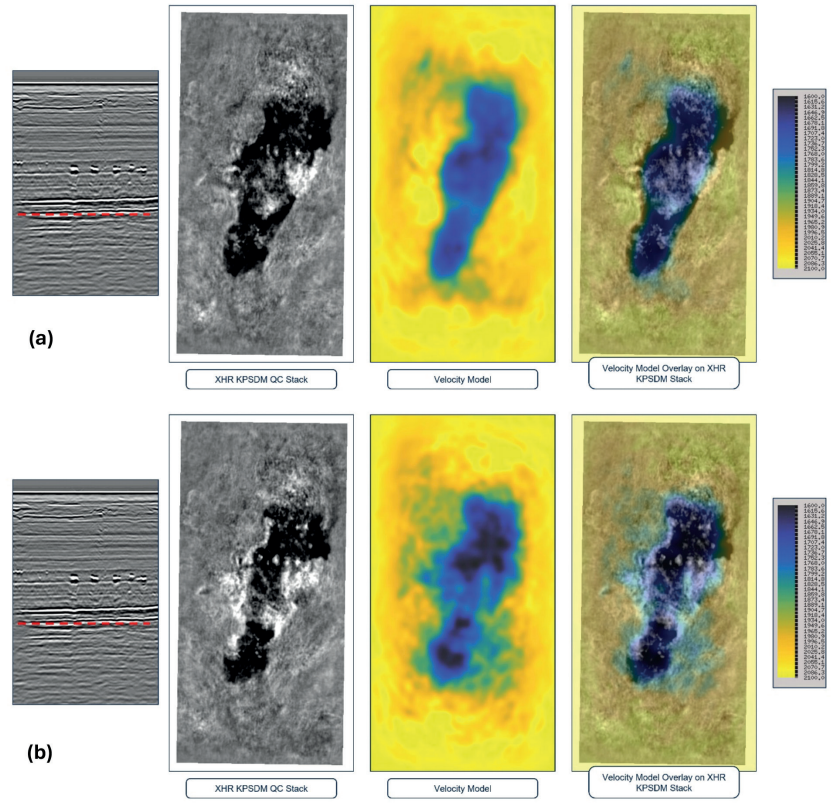

Figure 10 Time slices through KPSDM volumes of XHR data at depth 900 m: KPSDM using the 25Hz FWI-derived velocity model based on full hydrophone data (a), KPSDM using the 25Hz FWI-derived velocity model based on UDD data (b). Low velocities indicate the CO_2 plume.

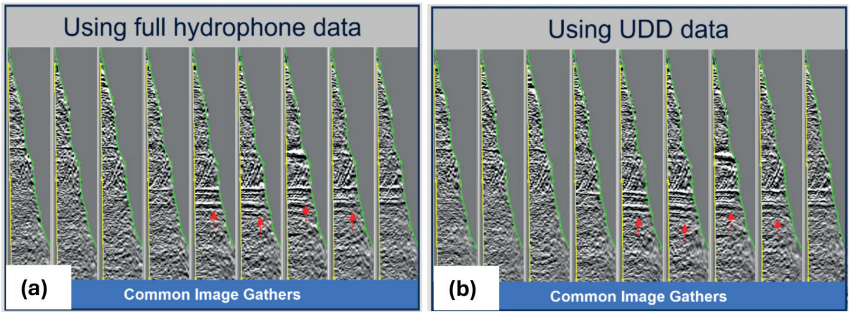

Figure 11 Image gathers: in the 25Hz FWI full wavefield hydrophone data derived velocity model (a) and in the 25Hz FWI UDD reflectivity data-derived velocity model (b).

and less-focused edges of the CO_2 plume. This is particularly evident on the depth slices (Figure 10). In the shallow area, the full hydrophone FWI results seem sharper compared to UDD FWI results, with less noise and with velocity updates that better follow the geology when comparing to the KPSDM stacks.

A second look shows that the UDD version exhibits fast velocity bands around the CO_2 plume, which are less dominant in the full wavefield results using hydrophone data. Common image gathers based on the UDD FWI model show downward curving gathers, indicative of a too fast velocity estimation in this area. In contrast, gather flatness using the FWI model based on the full hydrophone data version is significantly better (Figure 11).

Increasing frequency and wavenumbers: 60Hz FWI image compared to 60 Hz KPSDM image of short streamer data

The primary objective of the OBN data acquisition was to derive a velocity model to migrate the XHR data.

This was achieved by the 0-25Hz FWI-based velocity model derived on the full hydrophone data, as evidenced by the flat image gathers in Figure 12 a. However, we also wanted to investigate the maximum resolution achievable with FWI on this sparse nodal data set, so we carried on with the FWI work, beyond what is normally needed for a migration velocity model.

We continued to use the full wavefield and the data reconstruction method in the following FWI updates.

By replacing the field signature with a synthetic source, we shaped the wavelet in the data for each FWI frequency band. This can help in multi-scale FWI strategies by making the transition to higher frequencies smoother. By absorbing the near surface effects, the data reconstruction method prevents noise from getting imprinted in the shallow updates. Having cleaner updates in the shallow subsurface improves the results for deeper targets.

The frequency bands used for high-frequency FWI were 0-35 Hz, 0-45 Hz and 0-60 Hz. In addition to scaling up the frequency, we also scaled up the wavenumbers by increasing the contribution of smaller angles in the inversion. As for higher-frequency bands, at the 60 Hz stage, all angles were used.

The 60 Hz FWI-derived velocity model and its FWI image were compared with a depth-migrated UDD section and

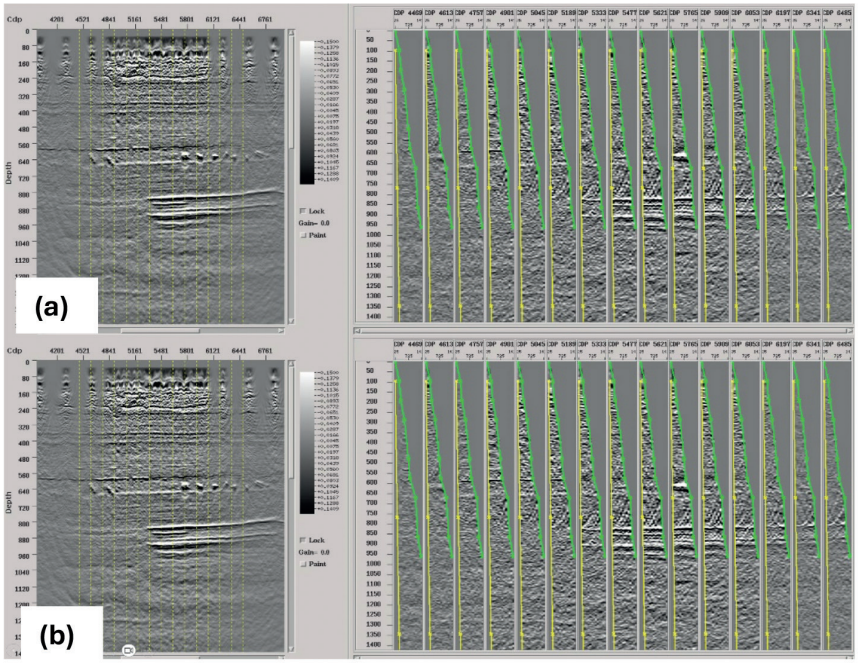

Figure 12 KPSDM stacks and image gather comparisons: 25Hz FWI velocity model based on full hydrophone data (a) and 35Hz FWI velocity model based on full hydrophone data (b) show hardly any differences, as expected.

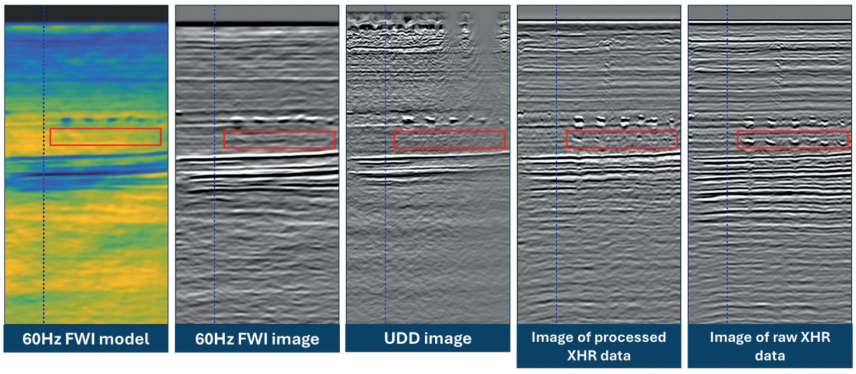

Figure 13 Migrated stacks showing multiple contamination on XHR images, which are far less prominent on the FWI velocity model and its derivative.

depth-migrated XHR data. In order to assess and validate the velocity model the raw migrated XHR data is also included in the comparisons (Figure 13). The raw XHR image contains clear and strong multiples at the injectite level (see the red box in Figure 13). They can be observed on the processed XHR dataset as weaker residuals. As expected, the UDD image doesn't contain those. More interestingly, the multiples generated by the injectites are only vaguely visible in the FWI model and FWI image, and far less evident than in the XHR images. This reduced multiple contamination demonstrates the added value of using multiples in FWI-based velocity estimation. That said, the small residuals observed in the FWI results need to be further investigated. They are likely to depend on the water velocity and details of the water bottom.

FWI experiment on primaries-only dataset (without Free Surface)

To further evaluate the impact of free surface multiples in a sparse node and shallow-water setting, we conducted an additional test. A synthetic 'primaries only' dataset was created using the 60 Hz velocity model through acoustic finite difference modelling. An absorbing boundary was used at the free surface in order to obtain data with primaries only. Figure 14 c shows the data set obtained in this manner. In comparison, we show the observed data in Figure 14 a and the modelled synthetic primaries and multiples data in the 60 Hz FWI model in Figure 14 b. The results show good correlation with the observed data for the main events. The strong low-frequency content in the primaries-only synthetic data is due to the absence of a ghost effect.

A QC done on stacks confirms the feasibility of using the primaries-only modelled synthetic data. Figure 15 shows a stack comparison between the UDD stack and the primaries-only modelled synthetic stack data. By multiplying the two stacks, a section QC is produced, highlighting phase differences and any mismatch between the two. Again, the shallow area demonstrates the major differences. The rest of the section, including the CO_2 plume, remains quite similar.

This primary-only synthetic data went through an FWI sequence up to 8 Hz with an absorbing free surface condition. The results are shown in Figure 16, which shows the velocity models, UDD images and UDD image gathers at 8 Hz for both the full wavefield and the synthetic primaries-only data.

The velocity model from the primaries-only data showed regions of higher than expected velocity in the shallow section,

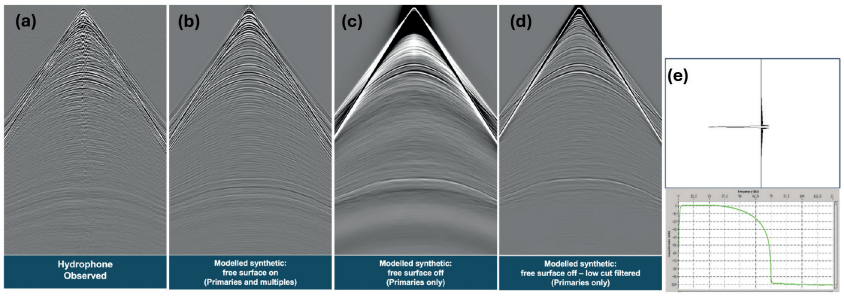

Figure 14 Observed hydrophone data (a), Modelled synthetic data obtained with the free surface on in the forward modelling (b), Modelled synthetic data obtained with the free surface off in the forward modelling (c), Low-cut fiiltered modelled synthetic data obtained with the free surface off in the forward modelling (d), wavelet used and its amplitude spectra (e).

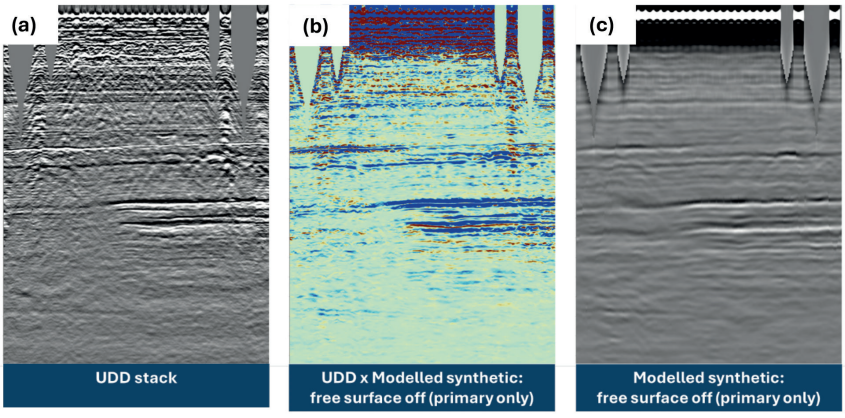

Figure 15 Up-Down Deconvolution stack (a), Modelled synthetic stack obtained with the free surface 'off' in the forward modelling (c) and multiplication result in (b) between the two – (a) and (c).

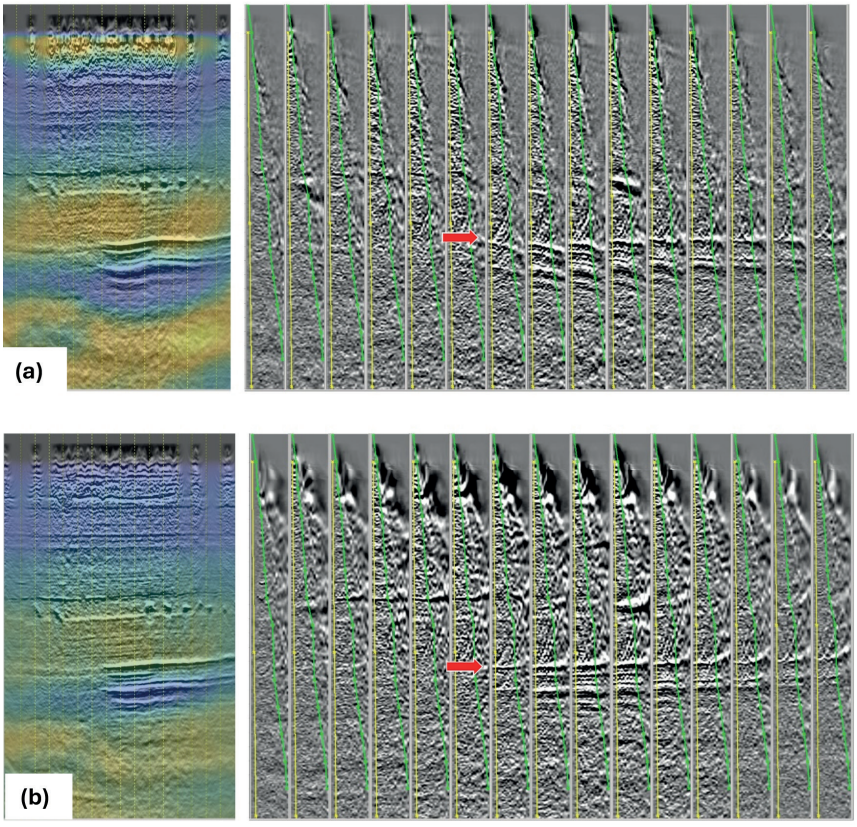

Figure 16 8Hz FWI Velocity model and common image gathers for the primary-only dataset route (a) and the full-wavefield hydrophone route (b).

highlighting the sparse node sampling imprint. Additionally, high velocities above the plume led to poor gather flatness in common image gathers (indicated by red arrows) and poor imaging with erroneous reflection events in the migrated stack. This underscores the advantage of using the full wavefield, which enhances shallow subsurface illumination through multiple energy, a benefit not achievable with primaries-only data.

Remaining challenges

In this section we discuss two remaining challenges with FWI on the sparse nodal data set.

The first one is that, although the 60 Hz FWI Image resolution at the CO_2 plume shows satisfying results to interpret nine sand layers, the overall resolution, particularly in the shallow area, is lower than the Kirchhoff PSDM image (Figure 17). This

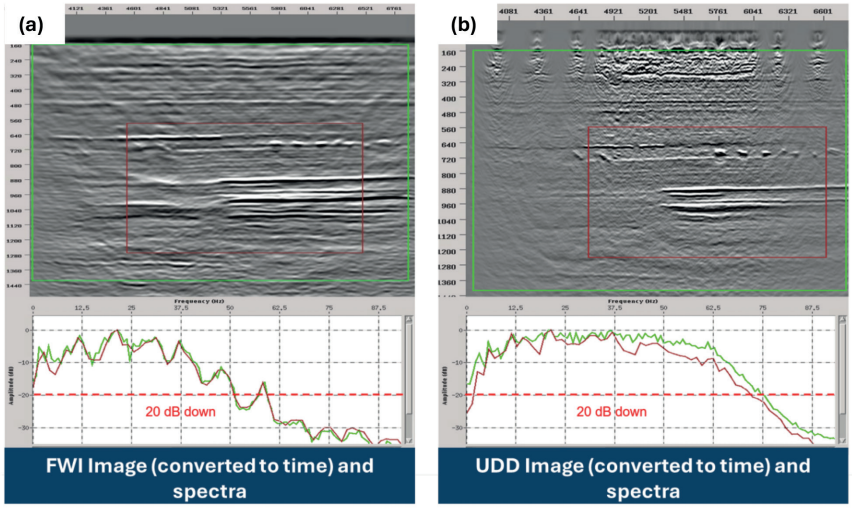

Figure 17 FWI Image derivative of the 60Hz FWI velocity model and amplitude spectra (a) and UDD KPSDM stack and amplitude spectra (b).

is mainly due to the regularisation (preconditioning to weigh the higher wavenumbers down) of the acoustic FWI gradient, which was used to avoid overfitting the data at high frequencies.

A second challenge is a questionable high velocity update, which can be observed just below the seabed and is probably an FWI artefact (Figure 18). To verify if this is a valid update, a travel time tomography has been run on the XHR data (Figure 19). A single pass of tomography was run, using the 8 Hz FWI velocity model displayed in Figure 8b. Due to the short offsets, limited pre-conditioning was applied to the gathers prior to RMO picking. Although the moveout is quite limited, the curvature-based picking worked successfully. However, updates are restricted to shallow depths because of the limited offset range in the short streamer data. Tomography was run down to 250 m.

The tomography run on the XHR data does not show the faster velocity in the shallow part and shows a different result than the FWI velocity model, with a decrease in velocity. Additionally, this is also observed on the XHR CDP gathers where events at this depth are dipping down slightly when the XHR data is migrated with the 60 Hz FWI velocity model. The CDP gathers are flatter when using the velocity derived by tomography on XHR data. PSDM QC on the XHR dataset shows stack improvements. This FWI artefact can be either due to elastic effects that were not fully mitigated by the data reconstruction method or to a lack of near-angle illumination, leading to unstable shallow velocity updates. Additional tests will be needed in order to accurately understand the origin of this FWI artefact.

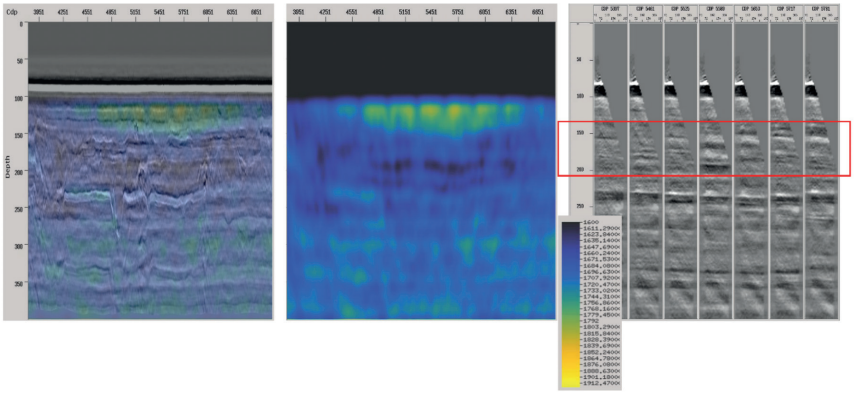

Figure 18 Zoom in the very shallow area showing the OBN 60Hz FWI velocity model overlaid on the XHR stack data and the corresponding XHR CDP gathers.

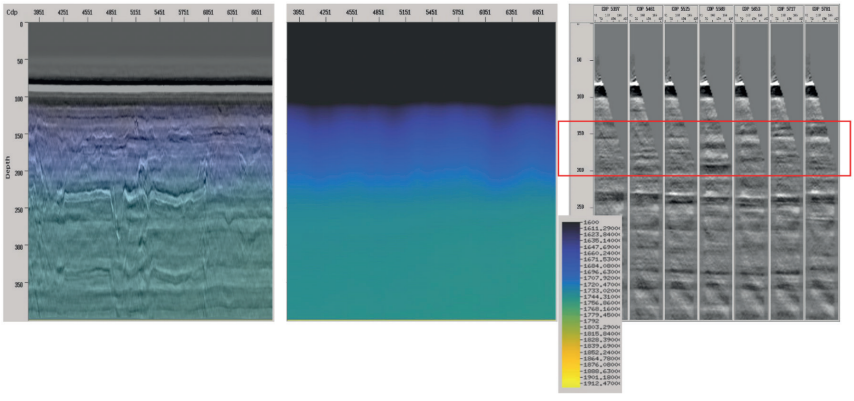

Figure 19 Zooming into the very shallow area showing the XHR travel time tomography-derived velocity model overlaid on the XHR stack data and the corresponding XHR CDP gathers.

Conclusions and way forward

Physical and cost constraints limit seismic acquisition configurations in CCS environments. Our study demonstrates the potential of overcoming these limitations by using short streamers and a cost-effective OBN operation together with the incorporation of multiples into the FWI process. The primary objective of this acquisition was to treat the datasets independently: XHR data provided a high-resolution image of the shallow subsurface and CO_2 plume, while OBN data provided a velocity model to depth migrate the XHR data. In addition, we have performed tests and assessments on the feasibility of FWI as a tool to provide a high-resolution velocity model and then to derive an interpretable volume from it.

By leveraging the full wavefield, we achieved a high-resolution velocity model update with a minimal number of nodes. This experiment confirmed that incorporating multiples enhances the accuracy and reliability of FWI-derived velocity models. We demonstrated that with FWI we managed to construct a kinematically correct velocity model and generated a high-resolution depth image from the XHR data. The resolution of the FWI velocity model was enhanced and its derivative indicates the method is on the right path with the FWI algorithm handling multiples well. However, the resolution of the final 60 Hz FWI image is lower than that of the 60 Hz KPSDM image from XHR data due to the lack of short offsets, or equivalently, small reflection angles.

An obvious way to try to increase resolution in FWI models and images is to include the XHR data in the inversion workflow. Ryan et al. (2024) performed an FWI on the XHR dataset only, using a regional velocity model as input. This led to high-resolution FWI models and images, but it could not update the kinematical content of the regional model because of the lack of offsets in the XHR data. In a CCS context, in order to provide correct imaging for each survey and hence an accurate monitoring, it is crucial to update the model, which underlines the need for a joint workflow – using OBN data for updating the model and the XHR data to improve the resolution of the FWI result, especially in shallow water, based on reflection data rich in high frequencies.

Another way to increase the resolution of FWI models and images based on nodal data only, would be to switch from acoustic to elastic FWI. This would allow us to move away from the kinematic approach adopted in DM FWI towards a dynamic one based on a least squares objective function. Modelling and using the amplitudes in a more correct manner is likely to help in increasing resolution. Elastic FWI may also avoid the shallow velocity artefact discussed in the previous section.

On the acquisition side, future operations can be more cost-effective by using smaller sources and smaller compressors, thereby reducing the equipment footprint. In a subsequent phase, decimation tests can also be performed to evaluate the impact of node and shot density on FWI results, consequently providing a reduced source and/or receiver effort to even further reduce the cost.

These advancements will unlock the potential for integrating OBN data into CCS projects, offering improved efficiency and accuracy in subsurface imaging and characterisation.

Acknowledgements

The authors would like to thank Equinor ASA and the CLIMIT program for their support and collaboration in the XHR/OBN Sleipner acquisition, as well as our colleagues at TGS and Equinor ASA for fruitful discussions and their support.

References

David, S., Zuberi, M.A.H., Cho, E., Baldock, S., Stokes, S. and Stock, G. [2023]. Unlocking Advanced Imaging for CCS Using Cost Effective Acquisition Solutions. *4th EAGE Global Energy Transition Conference and Exhibition,* Extended Abstracts.

Dehghan-Niri, R., Pedersen, Å.S., David, S., Westerdahl, H., Thompson, M., Furre, A-K., West, P. and Holm-Trudeng, T. [2023]. Proving the potential; monitoring Sleipner-CO2 plume with mini-streamers. *84th EAGE Annual Conference & Exhibition.*

Dehghan-Niri, R., Thompson, M., Mispel, J., Zarifi, Z., Gram, C., Olsen, P.A., Pedersen, Å.S., Ringrose, P., Furre, A.-K. and H. Westerdahl, H. [2022]. Optimizing a Geophysical Monitoring Toolbox for Offshore CO2 Storage. *16th International Conference on Greenhouse Gas Control Technologies, GHGT-16.*

Furre, A-K., Eiken, O., Alnes, H., Nesland Vevatne, J. and Kiær A. [2016]. 20 Years of Monitoring CO_2-injection at Sleipner. *13th International Conference on Greenhouse Gas Control Technologies, GHGT-13.*

Huang, Y., Mao, J., Sheng, J., Perz, M., He, Y., Hao, F., Liu, F., Wang, B., Yong, S.L., Chaikin, D., Citlali, Ramirez A., Hart, M. and Roende, H. [2023]. Toward high-fidelity imaging: Dynamic matching FWI and its applications. *The Leading Edge.*

Huang, Y., Mao, J., Xing, H. and Chiang, C. [2020]. Noise strikes, but signal wins in Full Waveform Inversion. *SEG 90th Annual Meeting.*

Mao, J., Sheng, J., Huang, Y., Hao, F. and Liu, F. [2020]. Multi-Channel dynamic matching full-waveform inversion. *SEG 90th Annual Meeting.*

Mispel, J., Furre, A-K., Sollid, A. and Maaø, F.A. [2019]. High Frequency 3D FWI at Sleipner: A Closer Look at the CO2 Plume. *81st EAGE Annual Conference & Exhibition.*

Quirk, D., Underhill, J., Gluyas, J., Wilson, H., Hiwe, M. and Anderson, S. [2021]. The North Sea through the energy transition. *First Break,* technical article.

Ringrose, P. [2018]. The CCS hub in Norway: some insights from 22 years of saline aquifer storage. *International Carbon Conference 2018.*

Ryan, C., Liao, K., Moore, H., Westerdahl, H., Thompson, M.,Pedersen, Å.S., Mispel, J., Wierzchowska, M., Dehghan-Niri, R. and Biryaltseva, Y. [2024]. Short Streamer Acquisition – the Potential and the Challenges. *3rd EAGE Geoscience Technologies and Applications Conference.*

Zuberi, M.A.H, Cho, E., Seher, T. and Myklebust, R. [2023]. Mitigating the effects of guided waves in OBN data for acoustic FWI using data reconstruction: A data example from the Yggdrasil area. *IMAGE 2023*, extended abstract.

Zuberi, M.A.H., and Pratt, R.G. [2018]. Mitigating nonlinearity in full waveform inversion using scaled-Sobolev pre-conditioning. *Geophysical Journal International*, **213**(1), 706-725.